A Differential Equations Model for the Ovarian Hormone Cycle

Steven M. Boker
Department of Psychology
The University of Virginia

Michael C. Neale
Departments of Psychiatry and Human Genetics
Virginia Commonwealth University

Kelly L. Klump
Department of Psychology
Michigan State University

Preprint of chapter to appear as
Boker, S. M., Neale, M. C. & Klump, K. L. (in press) A Differential Equations Model for the Ovarian Hormone Cycle. In *Handbook of Relational Developmental Systems: Emerging Methods and Concepts*, P. C. Molenaar, R. Lerner, & K. Newell (Eds). New York: John Wiley & Sons

Abstract

Dynamical systems models of behavior and regulation have become increasingly popular due to the promise that within–person mechanisms can be modeled and explained. However, it can be difficult to construct differential equation models of regulatory dynamics which test specific theoretically interesting mechanisms. The current chapter uses the example of ovarian hormone regulation and develops a model step by step in order for the model to be able to capture features of observed hormone levels as well as to link parameters of the model to biological mechanisms. Ovarian hormones regulate the monthly female reproductive cycle and have been implicated as having effects on affective states and eating behavior. The three major hormones in this system are estrogen, progesterone, and lutenizing hormone. These hormones are coupled together as a regulatory system. Estrogen level is associated with the release of lutenizing hormone by the hypothalamus. Lutenizing hormone triggers ovulation and the transformation of the dominant follicle into the corpus luteus which in turn produces progesterone. A differential equations model is developed that is biologically plausible and produces nonlinear cycling similar to that seen in a large ongoing daily-measure study of ovarian hormones and eating behavior.

Introduction

Recently there has been great interest in understanding developmental, behavioral, and physiological processes from a dynamical systems point of view. One benefit of studying processes as dynamical systems is that data are analyzed as person–specific and only subsequently modeled for sources of individual differences. This is a critical point — as students of human development and behavior we wish our findings not only to apply to population aggregates, but also to represent the complex patterns and etiologies exhibited by individuals as they develop and behave within their life context.

Underlying dynamical systems methods are statistical models that treat change as the fundamental concept of interest and data that are intensively sampled in time over multiple individuals (Boker, 2012). Statistical models for dynamical systems represent the time–dependency of data as the fundamental individual characteristic (Boker, Molenaar, & Nesselroade, 2009). That is to say, one does not so much make a model of what happened at a particular time as a model of what would have happened given some knowledge about previous states and context. In plain terms, dynamical systems models are not so much concerned with *what* happened as they are with *how* it happens.

Dynamical systems models are frequently considered within the theoretic framework of regulation. Thus a central concept is the idea of equilibrium — the time–dependency of a system is relative to its equilibrium (Boker, 2013). An equilibrium can be a single point, a cyclic figure such as a circle, or have more complex shapes. The behavior of a system as it regulates itself with respect to its equilibrium is termed the *basin of attraction* of a system. The shape of the attractor for a system will place constraints on a minimum set of model equations that can represent the dynamics of a system. Thus, visualizing the attractor for a system is often a first step to model specification as it can place constraints on model choice.

One technique that is frequently employed for visualizing attractors is called *phase space reconstruction*. Most techniques for phase space reconstruction involve some form of *time delay embedding*. This technique encapsulates the time–dependency within short time segments of observed data. An advantage of this method is akin to nonparametric smoothing: One need not make long–term assumptions about the behavior of a system. Instead, one uses short intervals of a few measurements at a time as local measures of the overall manifold of the dynamic. By assuming that the system can be captured locally by a smooth function, e.g., a parabolic basis function, one can recapture the overall geometry of the attractor — the long–term regulatory dynamics defined by the relationships between the derivatives of the attractor manifold (Takens, 1985; Whitney, 1936) — even when the long–term dynamics are not well described by a simple parabolic basis.

In order to make these abstract notions more concrete, example data from a study

---

Funding for this work was provided in part by NIMH Grant MH082054–01, NIH Grant 1R21DA024304–01, and the Max Planck Institute for Human Development Lifespan Psychology Group. Any opinions, findings, and conclusions or recommendations expressed in this material are those of the authors and do not necessarily reflect the views of the National Institutes of Health or Max Planck Society. Correspondence may be addressed to Steven M. Boker, Department of Psychology, The University of Virginia, PO Box 400400, Charlottesville, VA 22903, USA; email sent to boker@virginia.edu; or browsers pointed to http://people.virginia.edu/˜smb3u.

of relationships between ovarian hormones and eating behavior will be presented. Reconstructed attractors for estradiol and progesterone will be plotted and discussed. Next, modeling choices will be made in order to create a biologically plausible differential equations model for estradiol and progesterone. Finally the model will be numerically integrated and will be compared to the reconstructed attractor from the data for one individual. This is only a first step to understanding these data, but statistical parameter estimation of a multilevel model for the ovarian hormone cycle with proper treatment of individual differences is beyond the scope of this introductory chapter. Instead, let us focus our attention on how one develops a dynamical systems model suitable for later statistical testing.

All too often, statistical models are chosen because they have been useful in other applications, a case of everything looking like a nail to someone holding a hammer. This chapter strongly recommends that models be developed to serve explanatory function by tying the dynamics of the model to what is known about the micro– and/or macro–structure of the processes of interest. With this view in mind, we will reconstruct empirical attractors for estradiol and progesterone as estimates of the macro–structure of the process and use biological details of the ovarian cycle to inform the micro–structure.

The Example Hormone Data

The data we will use as an example is a small sample ($N = 4$) from a much larger ($N = 238$) twin study of eating behavior and ovarian hormones in normally menstruating young (age $\mu = 17.9$, $\sigma = 1.7$) women (Klump et al., 2013). In order for participants to be included in the study they met the following criteria: i) menstruation every 22–32 days for the past 6 months; ii) no hormonal, psychotropic or steroid medications within the past 8 weeks; iii) no pregnancy or lactation within the past 6 months; and iv) no history of genetic or medical conditions known to influence hormone functioning or appetite/weight. The sample of four individuals were selected specifically to exemplify the diversity of patterns of hormones observed in the larger study.

Saliva samples were collected every morning for 45 consecutive days within 30 minutes of waking. Daily estradiol and progesterone levels were measured by enzyme immunoassay (see Klump et al., 2013, for details). Time series plots of normalized hormone levels and self–reported days of bleeding for the four selected example participants are shown in Figure 1. Two observations are immediately apparent from these plots: There are substantial individual differences in the cycles as well as substantial intraindividual variability within the major cyclic pattern. Of particular interest is the apparent 5 day cycle of estradiol in Figure 1. This rapid cycle in estradiol levels was observed in a substantial fraction of women in the study.

Phase Space Reconstruction

In order to plot a phase space reconstruction of an attractor from time series data, the time series must first be converted into a time delay embedded matrix. In the most commonly used methods, two integers are chosen: a delay parameter, τ, and a dimension, D, and the time series (e.g., a vector with P elements) is then converted to a $P - D \times D$ matrix where each column of the matrix is lagged by τ elements from the previous column (Sauer, Yorke, & Casdagli, 1991) as shown in Equation 1. When using this method, *tau* is

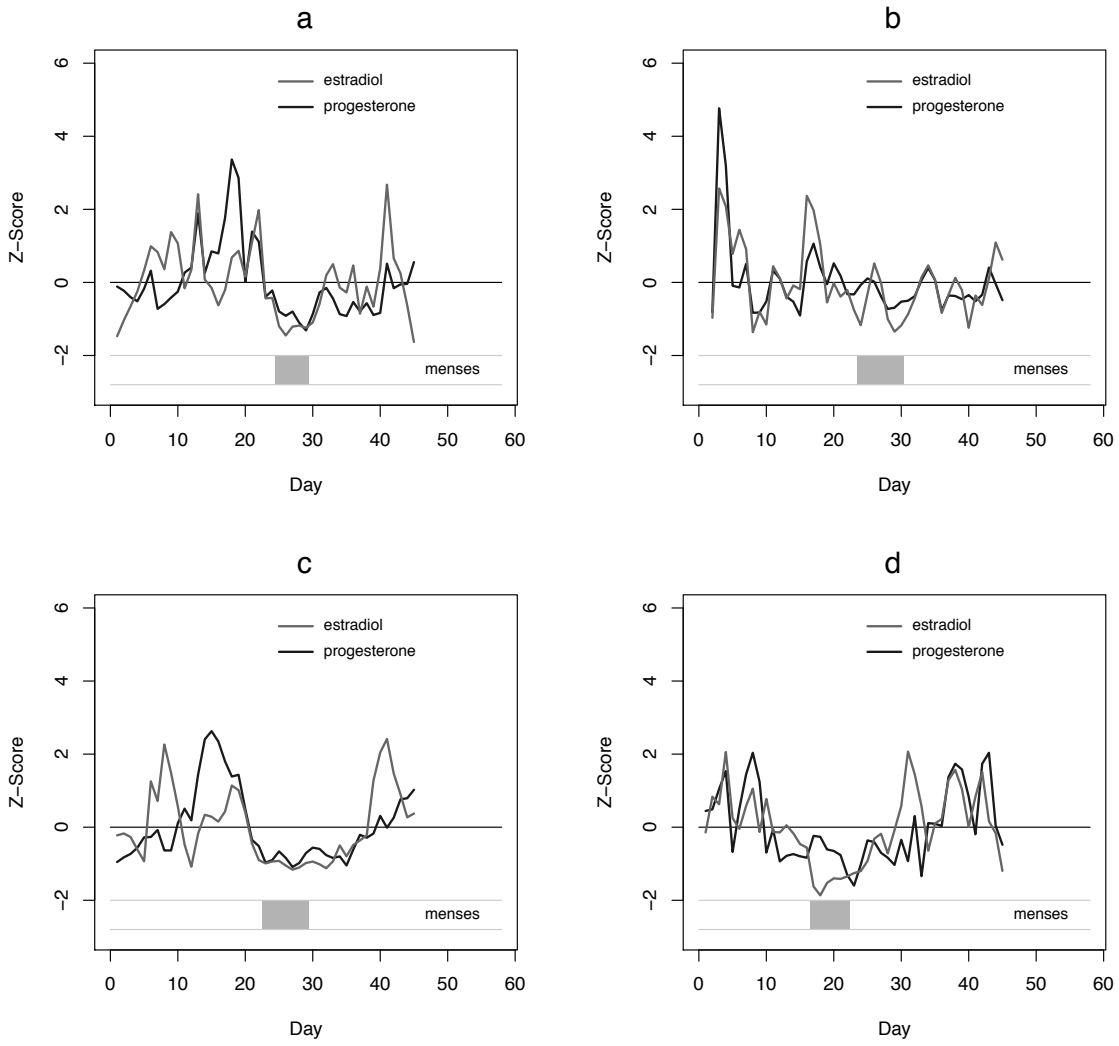

Figure 1. Time series plots of estradiol and progesterone Z–scores for four selected example participants.

chosen so as to spread the attractor out in the D dimensional state space. In the case of a linear cyclic attractor with a wavelength λ, the optimal value would be $\tau = \lambda/4$ (Takens, 1985). Various methods are used to choose τ, the most common of which are the first zero crossing of the autocorrelation and the first minimum of the average mutual information (Abarbanel, Brown, & Kadtke, 1990; Kennel, Brown, & Abarbanel, 1992). Once the data are time delay embedded, they are typically displayed as a scatter plot where, for instance the first column of the time delay matrix, $x(t)$, is represented by the horizontal axis and the second column, $x(t+\tau)$, by the vertical axis. This creates what is termed a *state space plot* since D-dimensional states of the system are directly plotted.

The advantage of a state space plot is that it preserves the fine grained structure of the system. However, in data of interest in human dynamics, there is frequently a mixture of time–independent measurement error and time–dependent dynamics. By using a locally parabolic (or higher order Taylor series) filter, time derivates of a time series can be estimated (Savitzky & Golay, 1964) while creating a local smoothing of the data to separate time–independent noise from the time–dependent dynamics. A recently developed method for performing this task uses Generalized Orthogonal Linear Derivative (GOLD) (Deboeck, 2010) weights for Generalized Local Linear Approximation (GLLA) (Boker, Deboeck, Edler, & Keel, 2010). This method estimates derivatives for each measurement in a time series and then these derivatives can be plotted as a *phase space plot*.

In order to use the GLLA method, a time delay embedded matrix must be constructed, and thus the quantities τ and D must still be chosen. However, these choices follow a somewhat different logic than does the state space reconstruction method. The reasons for this are twofold: i) the choice of the order of the highest derivatives to estimate is decoupled from the choice of D in the time delay embedding; and ii) the choice of τ and D contribute to the degree of smoothing applied to the time series. The details of these two choices will be treated more comprehensively in a moment, but first we will explicitly define the construction of a time delay embedded matrix and its associated GLLA filter for estimating derivatives.

Time Delay Embedding

Suppose a time series with P elements, $X = \{x(1), x(2), x(3), \ldots, x(P)\}$. Suppose further that we choose a time lag, τ and dimension, $D = 5$. A time delay embedded matrix, which we will designate $\mathbf{X}^{(5)}$, can be constructed as

$$\mathbf{X}^{(5)} = \begin{bmatrix} x_{(1)} & x_{(1+\tau)} & x_{(1+2\tau)} & x_{(1+3\tau)} & x_{(1+4\tau)} \\ x_{(2)} & x_{(2+\tau)} & x_{(2+2\tau)} & x_{(2+3\tau)} & x_{(2+4\tau)} \\ x_{(3)} & x_{(3+\tau)} & x_{(3+2\tau)} & x_{(3+3\tau)} & x_{(3+4\tau)} \\ \vdots & \vdots & \vdots & \vdots & \vdots \\ x_{(P-1-4\tau)} & x_{(P-1-3\tau)} & x_{(P-1-2\tau)} & x_{(P-1-\tau)} & x_{(P-1)} \\ x_{(P-4\tau)} & x_{(P-3\tau)} & x_{(P-2\tau)} & x_{(P-\tau)} & x_{(P)} \end{bmatrix}. \quad (1)$$

Note that time–dependency from the time series X is now represented as multiple short samples in the rows of $\mathbf{X}^{(5)}$. Thus, when we estimate derivatives of the time series, each row can contribute a new estimate of the covariance between these time derivatives. This is an important point — we have *localized* the time derivative estimation over the manifold

of the attractor without committing to any particular model for the whole attractor. This is true of any method that uses time delay embedding.

The GLLA method uses a power series approximation to extract the time–dependency in each row of the time delay embedded matrix. Suppose we construct a basis function matrix L in a manner similar to the fixed loading matrix for a latent growth curve model such that the first column of L are the loadings to estimate the latent intercept, the second column of L estimates the latent first derivative (slope), and the third column of L estimates the latent second derivative (curvature). For the $D = 5$ time delay embedding example above, L would be

$$\mathbf{L} = \begin{bmatrix} 1 & -2\Delta t\tau & (-2\Delta t\tau)^2/2 \\ 1 & -1\Delta t\tau & (-1\Delta t\tau)^2/2 \\ 1 & 0 & 0 \\ 1 & 1\Delta t\tau & (1\Delta t\tau)^2/2 \\ 1 & 2\Delta t\tau & (2\Delta t\tau)^2/2 \end{bmatrix} \tag{2}$$

The first column of L is a basis function for an intercept. The second column of L is a basis function for a unit value linear slope where the elapsed time between successive columns of $\mathbf{X}^{(5)}$ is τ times the elapsed time Δt between successive observations of X. The third column is the indefinite integral of the second column. Now, if the zeroth, first, and second derivatives of X were in the first, second, and third columns of a $P - 4\tau \times 3$ matrix Y, then

$$\mathbf{X}^{(5)} = \mathbf{Y}\mathbf{L}' + \mathbf{E} \tag{3}$$

If $\mathbf{L}'\mathbf{L}$ is nonsingular, then the right quasi–inverse $\mathbf{W} = \mathbf{L}(\mathbf{L}'\mathbf{L})^{-1}$, is a least–squares solution such that

$$\mathbf{Y} = \mathbf{X}^{(5)}\mathbf{W} \, . \tag{4}$$

Thus, we can obtain least squares estimates of the derivatives of X with a single matrix multiplication if $\mathbf{W}$ is known. An R function to calculate $\mathbf{W}$, given choices for D, τ, and Δt is available online at `http://people.virginia.edu/~smb3u/GLLAfunctions.R` (Deboeck's GOLD function can be found in Deboeck, 2010).

Choosing τ and D for GLLA Derivative Estimation

When using GLLA to estimate derivatives, the first question is, "What is the highest order derivative to estimate?" Zeroth order derivatives will just estimate a polynomial smooth of your time series and store it in a column vector. Zeroth and first order derivatives will estimate a polynomially smoothed time series along with a smoothed first derivative time series and store it into a matrix with two columns. Zeroth, first, and second order derivatives adds a column for the second derivative to the output matrix, and so on. In practice, it is rarely useful to estimate less than second order derivatives even if you only use the first two columns of the resulting matrix. Note that a first order autoregressive process can be transformed into a first order differential equation and so you would need zeroth and first derivatives at a minimum. If the process of interest has fluctuations or oscillations, a second order differential equation is the minimum order that can represent oscillations.

The next question to ask is, "What is the minimum amount of time that elapses in one complete oscillation or fluctuation?" If the process of interest is a first order process,

e.g., growth that approaches but does not pass an equilibrium value, then it is safe to skip to the next paragraph. But if the process could oscillate or fluctuate around an equilibrium, then decide how long the time is, on average, between peaks. An easy way to do this is to use the autocorrelation function (acf) in R. The acf function will plot a graph that will show the autocorrelation for a series of lags in a time series. If one finds the first peak to the right of zero, the elapsed time as read on the horizontal axis of the plot will tell the elapsed number of samples on average from peak to peak. The lag in samples between the leftmost and rightmost column of the time delay embedded matrix must be less than the elapsed samples in the acf plot. Figure 2 plots the autocorrelation function for the four participants whose data were plotted in Figure 1. The minimum number of days for the autocorrelation peaks across all four participants is 12 days.

The last question to ask is, "How much smoothing should be applied when calculating the derivatives?" If one wishes to remove as much non–time–dependent information as possible, the total amount of elapsed time between the first and last columns of the time delay embedded matrix should be as long as possible, but of course shorter than the minimum fluctuation wavelength estimated above. If the time series is short, one may wish to modify that decision since the more time that is covered by the time delay embedded matrix, the fewer the number of rows that result. Notice that the number of rows in the matrix in Equation 1 is $P - (D\tau)$. So although the time series originally had P elements, the time delay embedded matrix only has $P - (D\tau)$ rows. As either D or τ become larger, the number of samples of the time dependency become smaller. So, one does not necessarily want to always make D and τ as large as possible.

In practice, it turns out that the total lag from the first column to the last column is what is most important for all of these problems. In general, we recommend to set $\tau = 1$ since this means that there is better noise rejection within each row of the time delay embedded matrix (For a discussion of how time delay embedding improves noise rejection, see Oertzen & Boker, 2010). Thus, the only choice that remains is setting D to be less than the minimum wavelength (in samples) of the time–dependent fluctuations of interest and for derivative estimation of order O, D should be greater than or equal to $O + 2$. This last restriction is so that there is at least one degree of freedom for smoothing.

In the ovarian hormones example, we wish to estimate a second order system ($O = 2$). In addition, we are primarily interested in an approximately monthly cycle, but the shorter cycles may be important too. Thus, we chose $\tau = 1$ and $D = 11$ so that we could still capture the 12 day cycles but had maximum smoothing within the 12 day period. In practice, one may wish to explore other choices for D to see if other shorter– or longer–period features are exposed.

Matrix Scatterplot of Phase Space

To prepare for phase space visualization, participants' hormone time series were normalized using their individual mean and standard deviation. The data were then time delay embedded using a lag of $\tau = 1$ and number of embedding columns $D = 11$. Zeroth, first and second order derivatives were estimated by the Generalized Local Linear Derivatives method (Boker, Deboeck, et al., 2010) using a Generalized Orthogonal Linear Derivatives (Deboeck, 2010) transformation matrix. The resulting derivatives for estradiol and progesterone for the four example participants are shown as matrix scatterplots in Figure 3. This

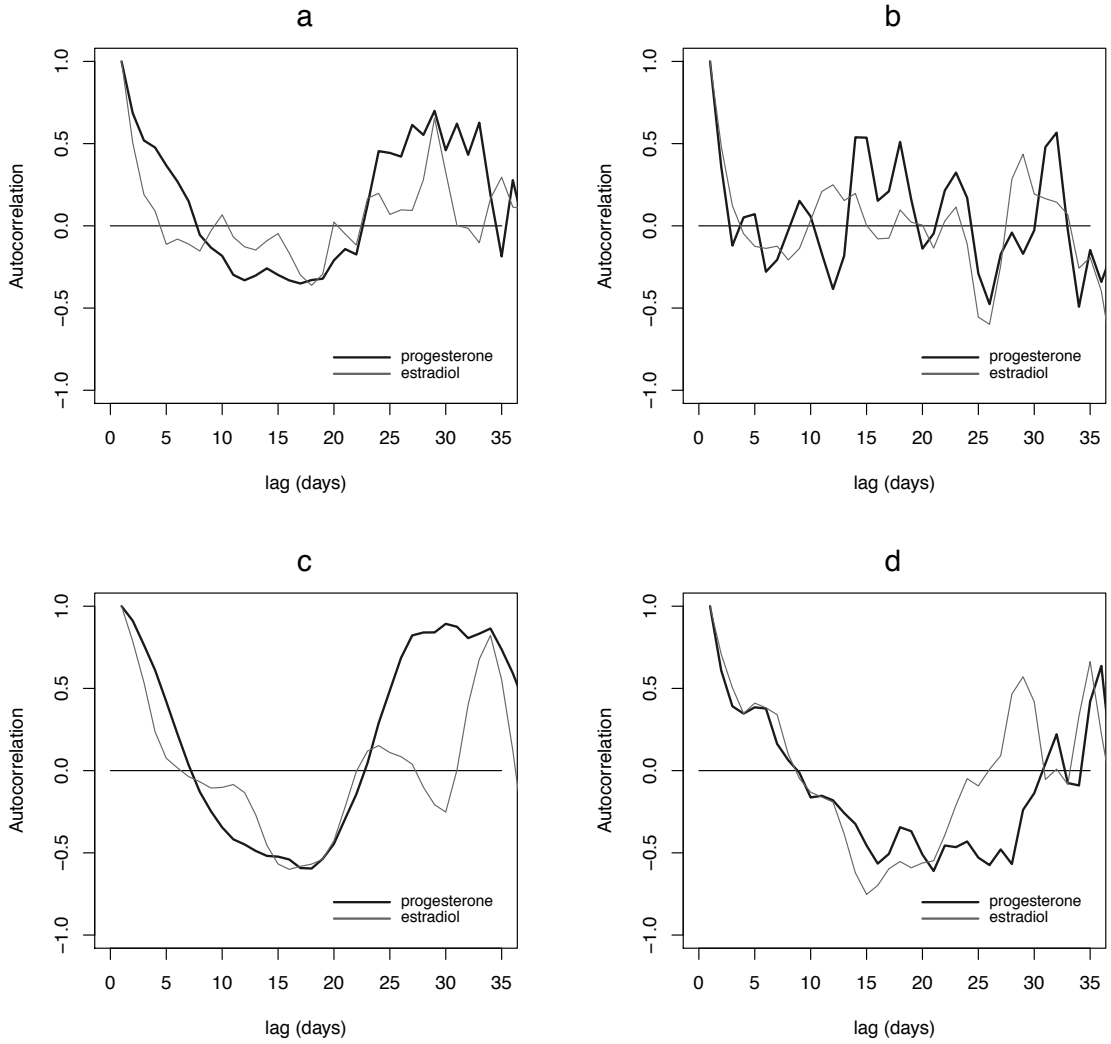

Figure 2. Autocorrelation plots of estradiol and progesterone for four selected example participants. (a) Main oscillation autocorrelation peak for both estradiol and progesterone at 29 days. (b) Noisy, but likely peaks for progesterone at 15 and 31 days and for estradiol at 12 and 30 days. (c) Easy–to–read peaks for progesterone at 30 days and for estradiol at 12, 24, and 35 days. (d) Peak for estradiol at 28 days and for progesterone at 35 days.

method plots each combination of derivatives against one another, including the derivative pairs for the cross coupling between estradiol and progesterone. Thus, not only is each within–variable reconstructed attractor visualized, but also the attractor formed by the cross coupled variables. Since this visualization is novel, we will next engage in a detailed explanation and interpretation of what is being displayed.

Figure 3 provides rich information about regulatory processes for estradiol and progesterone. We will begin by focusing on Figure 3-c. First, note that the relationship between almost all of the pairs of derivatives includes some sort of loop – an interior and an exterior. This is very different from a bivariate normal scatterplot! These loops are clear indicators of oscillation. However, if the process was a linear oscillator, we would expect to see ovals, circles, and perhaps lines. Instead, note that, e.g., the relationship between estradiol and the first derivative of estradiol (Est, dEst) looks like it has a spot where there are many dots overlaid as well as a regular loop. The relationship between estradiol and the first derivative of progesterone looks as if it is a figure eight. The relationship between the first and second derivatives of progesterone is heart–shaped, with an area that looks like many overlaid dots along with a long loop where the dots are spread out. Each of these observations leads to a conclusion that the regulatory system must include some nonlinear process.

If ovarian hormone regulation can be considered as a single system, then the individual's matrix plot in Figure 3–c displays only one attractor that exists in a higher dimensional space. However, we are looking at its shadow on the plot as if it were lit from from different perspectives. That is to say, the geometric figure in the higher dimensional space is projected down onto the 2–D surface of the plot. What does this higher dimensional figure look like? Is it possible that a relatively simple structure is being viewed from different angles and casts its shadow in a way that would reproduce all of these varied forms?

In order to answer that question, we will take a look at a concept from dynamical systems called *winding number*. Figure 4–a displays a system with a winding number of zero: the solid, straight black line plotted onto the top of the tube. This figure is a representation of an attractor for a linear system such as a univariate regression, there is one slope coefficient and it doesn't change over time. Now consider Figure 4–c. The solid line is now a circle. We have bent the tube around and joined its two ends to form a torus. This figure represents a sinusoidal oscillating system: the slope is first positive, then negative, then positive again. Imagine mentally rotating the torus so that you see the circle from various perspectives. It would cast the shadow of either a circle, an oval, or a line if you looked at it edge–on.

Next consider Figure 4–b. The solid line now spirals around the tube twice — a winding number of 2. If we perform the same trick of bending the tube and connecting the ends to form a torus (Figure 4–d), the black line spirals around the tube of the torus twice for each time it orbits the hole of torus. This figure represents an oscillating system with a winding number of two.

It is difficult to mentally rotate and project the shadow of the black line spiraling and orbiting on Figure 4–d, so six projections of that system are displayed in Figure 5. The projections of the black line spiraling and orbiting the torus are very similar to the those plotted in the empirical phase space reconstructions shown in Figure 3. It appears that a system with winding number 2 may be able to model the ovarian hormone data.

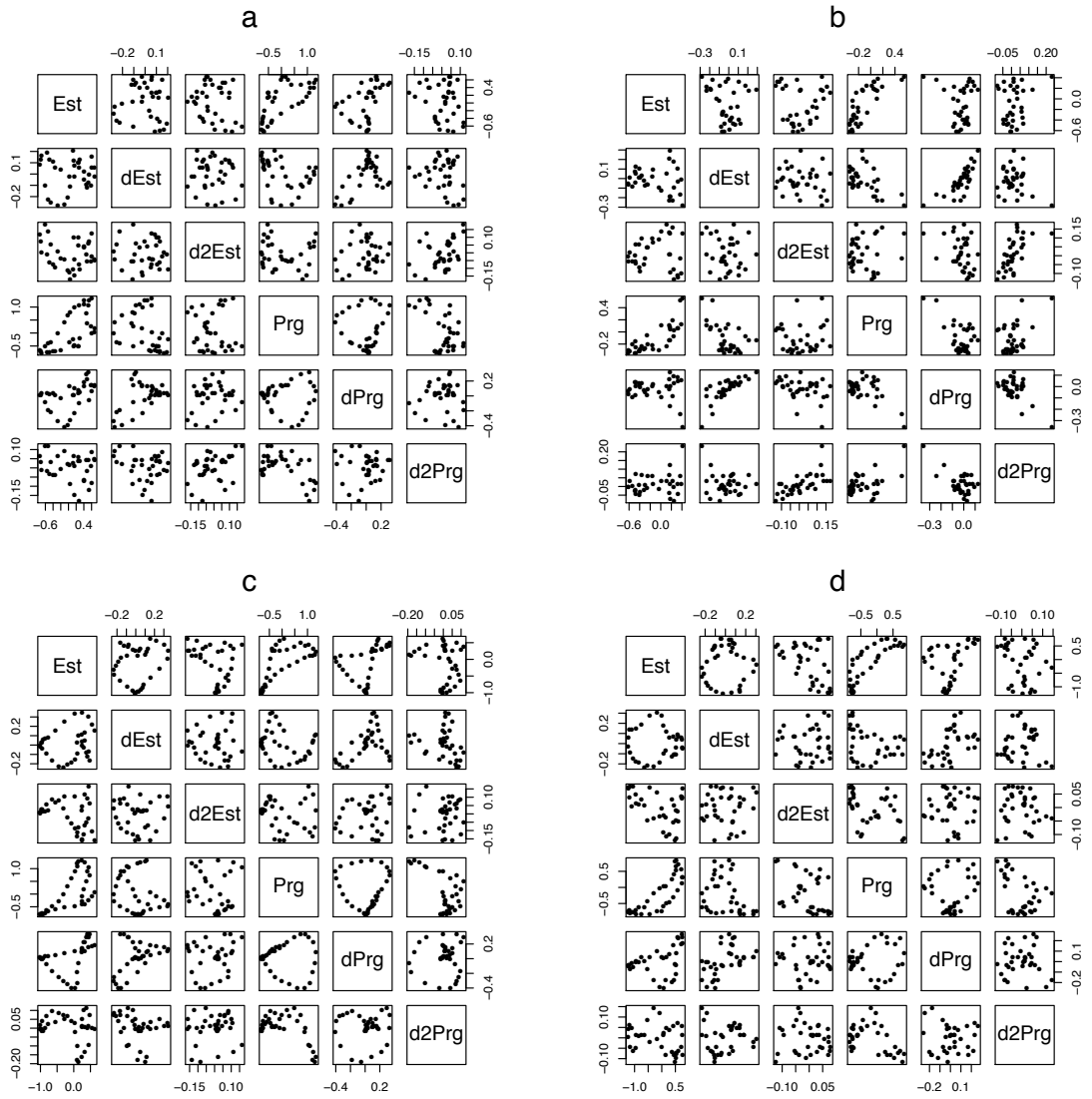

Figure 3. Scatterplot matrix of zeroth, first, and second derivatives for estradiol and progesterone from the four example participants. An example R script to produce this type of phase space reconstruction plot from time series is provided in Appendix A.

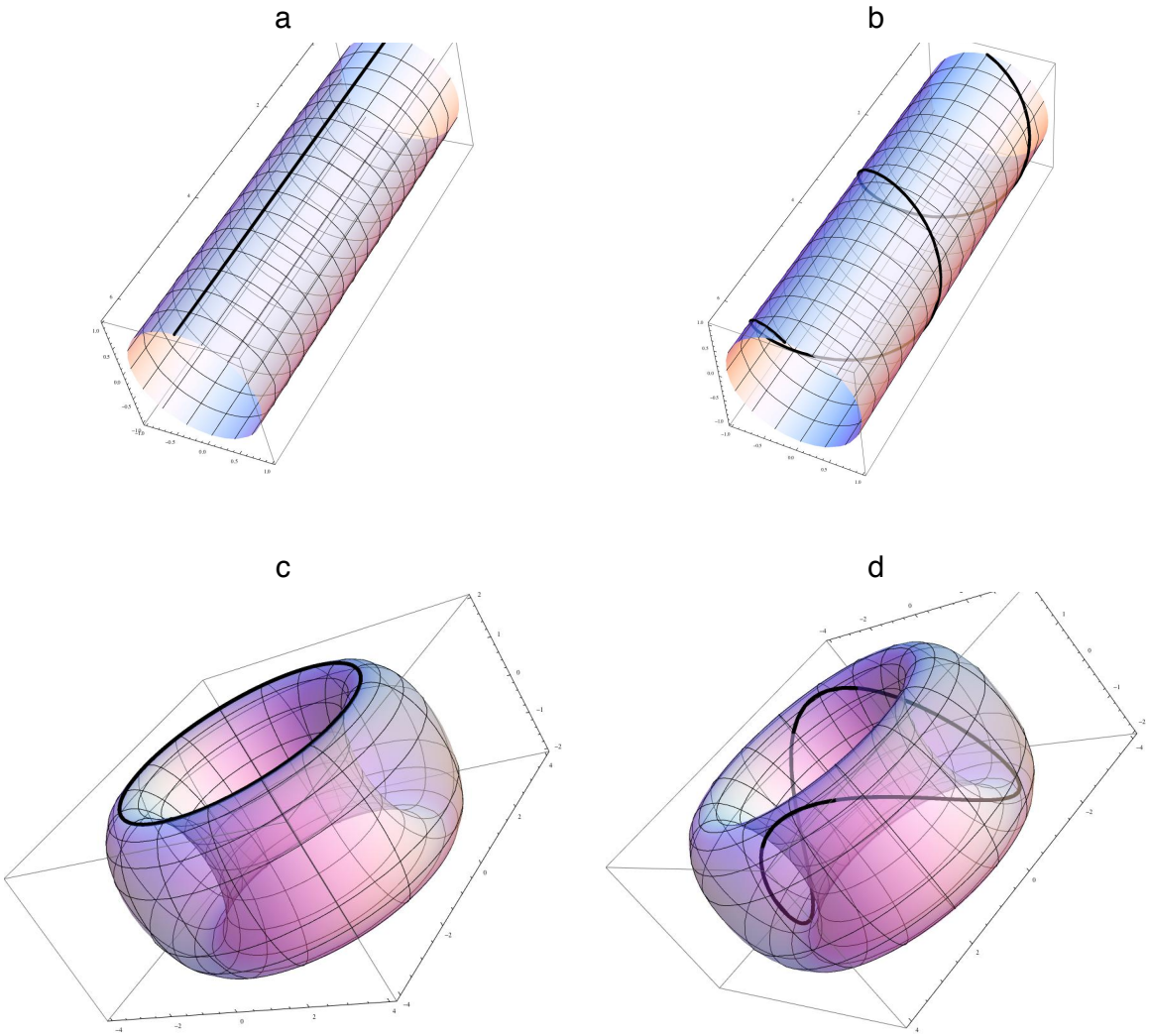

Figure 4. Visualization of winding numbers zero (a,c) and two (b,d). (a) A system with a winding number of 0 can be plotted as a straight line on a tube. (c) An oscillating system with a winding number 0 can be plotted as a circle around the hole in a torus. (b) A system with a winding number 2 spirals around the tube twice. (d) When the tube is turned into a torus, a system with winding number 2 spirals around the tube of the torus twice for each time it circles the hole in the torus.

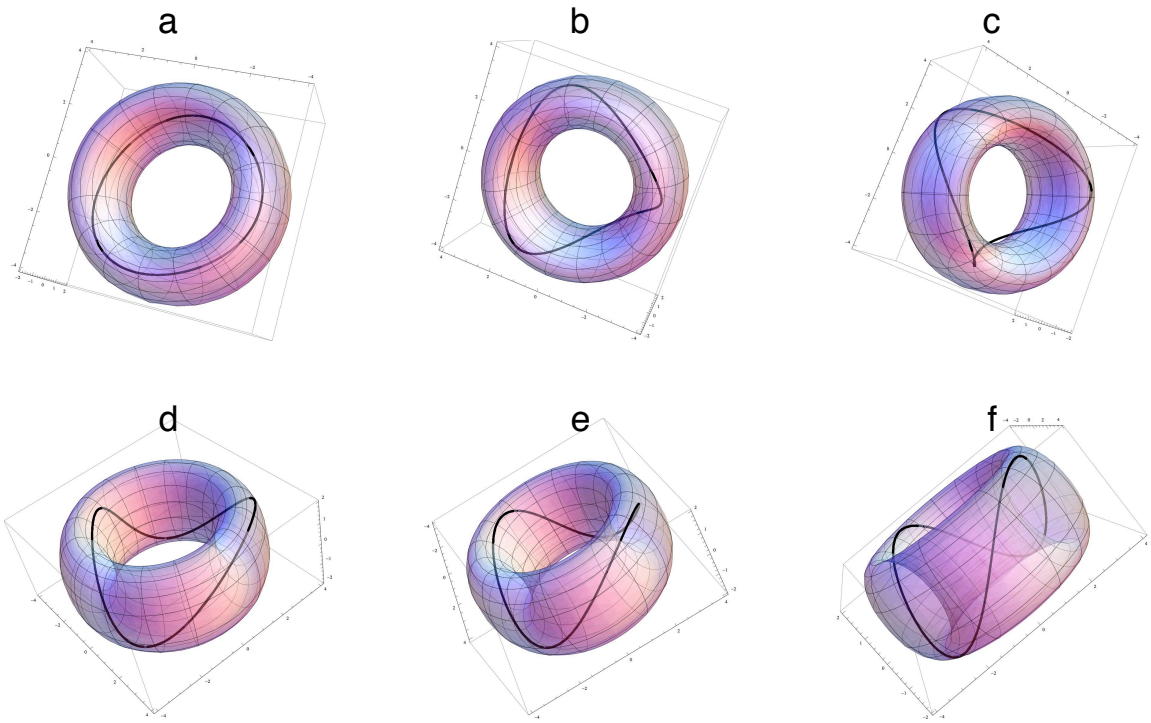

Figure 5. Six perspective views of the same trajectory: an oscillation with winding number 2. The trajectory makes two spirals around the tube of the torus for each orbit it makes around the hole in the torus. From each perspective, the black line of the trajectory appears to have a different shape.

Constructing a Dynamical Systems Model

If dynamical systems models are to be explanatory rather than merely descriptive, then the construction of models for phenomena are placed under constraints that are not merely data driven. In other words, constraints from theory and known mechanisms (from e.g., biology, genetics, or physics) must play a major role in constructing alternative models. There is no statistical test that optimally weights the contributions of theory, known mechanisms, and statistical fit to observed data so as to provide an objective measure for model selection. However, it does make sense to direct the model building process at the outset so as to include as many constraints as are well established so as to restrict the search for a statistically optimal model to the space of plausible explanatory models. Simply put, it may not useful to fit a model to data simply because it is easy. For instance, fitting a linear regression to time–intensive repeated measures of self–report hunger would likely result in a model with a significant non–zero intercept and a slope that was not distinguishable from zero — a prediction that everyone was moderately hungry all the time: clearly a nonsensical result.

So, how does one construct a dynamical systems model? First, it is important to realize that this will be a model for relationships between instantaneous time derivatives of variables and their equilibrium values. To continue the hunger example, one should ask,

"How does the current rate of change of hunger relate to the current displacement from equilibrium?" If one is more hungry than one's long term average (equilibrium) value for hunger, it is likely that a meal or snack will be in one's immediate future and thus hunger is likely to decrease as a result. Similarly, if one is less hungry than the equilibrium, it is likely that one will not be eating for some time — resulting in an increasing value for hunger. Thus, we predict a negative relationship between the current value of hunger and the current slope for hunger.

In practice, we have used three strategies for constructing dynamical systems models. First, we have used existing theories and intuition to list the plausible relationships between derivatives and built models from the resulting constraints as was begun in the preceding paragraph. This method can also be empirically driven in that features of the data, such as the phase space reconstructions plotted in Figure 3, can restrict the choice of models.

Second, we have looked closely at the language that is used to describe phenomena and tied descriptions of dynamic relationships back to models from physics. For instance, when articles describe a phenomenon such as resiliency in words like "bouncing back from adversity," (Ong, Bergeman, & Boker, 2009) we have taken these dynamic metaphors seriously and constructed and tested models for elasticity (Boker, Montpetit, Hunter, & Bergeman, 2010). Or when a rapid change in mood is described as a "mood swing", we have looked to physical models of pendulums and momentum (Bisconti, Bergeman, & Boker, 2004; Boker, Leibenluft, Deboeck, Virk, & Postolache, 2008).

The third way we have constructed models is by implementing physiological or biological constraints in order for the model to be biological plausible and for its parameters to map to physical processes. We will use a combination of the first and third methods to construct a differential equations model of the ovarian hormone cycle. With that in mind, the next section describes some of the known biology involved in the production and regulation of ovarian hormones.

Constraints from Biology

The human menstrual cycle has three characteristic hormones (estrogen, luteinizing hormone, and progesterone) that are functionally involved in ovulatory regulation. The menstrual cycle is divided into two phases and sometimes subdivided further. The follicular phase begins at the onset of menstrual bleeding and ends at ovulation. The luteal phase then begins after ovulation and ends at the onset of menstrual bleeding. Ovulation is considered to be a phase in itself. Some refer to the luteal phase as the premenstrual phase while others define a separate premenstrual phase as a shorter period at the end of the luteal phase. Menstrual bleeding lasts an average of 5 days and 90% of menses are within the range 3 to 8 days (Fehring, Schneider, & Raviele, 2006). The mean interval between subsequent onsets of menses (menstrual cycle length) has been estimated to be between 28 (Munster, Schmidt, & Helm, 1992) and 29 days (Fehring et al., 2006), but the variability in this estimate is large. Estimated within–person cycle–to–cycle variability (approximately 40% of women have more than 7 days intracycle variability) is nearly as large as the between–person individual differences (approximately 22–35 days 95% confidence interval) in cycle length (Fehring et al., 2006; Geirsson, 1991; Munster et al., 1992). This large variability in cycle length provides another hint that substantial nonlinearity is present in this regulatory system.

Figure 6 plots mean curves of normalized progesterone, estradiol, and LH levels and their associated 90% confidence intervals from a daily measurement norming assay study (Stricker et al., 2006). Each of these plots is centered around the peak of LH being at day 15. Timing variability in these plots is represented by the shaded gray areas. In Figure 6–b, note the large uncertainty as to the timing of the peak of LH represented by the large gray area from day 10 to 22. This graphically presents the observed variability in the length of the follicular phase (Fehring et al., 2006). The graphs of estradiol and progesterone also show this large timing uncertainty due to the uncertainty in timing of the LH peak. Timing variability in the individual data curves that were averaged to produce the mean curves results in substantial smoothing and could hide high frequency within–person fluctuations that may be present in the individual–level data.

After the end of menses, ovarian follicles are stimulated to grow, one of which will subsequently mature. As the follicles develop, they release estradiol and levels of estradiol begin to rise. Once estradiol passes a threshold, it triggers a quick rise in luteinizing hormone, a phenomenon known as the LH surge. The mechanism for this in humans has not been well established, but evidence from animal models suggests that there are two receptors in the hypothalamus known as estrogen receptor–α and receptor–β that are involved (Hu et al., 2008). According to this view, low levels of estrogen activate estrogen receptor–α in a negative feedback loop which in turn suppresses the production of LH. But once estrogen has risen above a threshold, a positive feedback mechanism is triggered by β–receptors in the hypothalamus which produces LH. The positive feedback means that there is rapid exponential growth in LH over an interval of hours — the LH surge. This combination of positive and negative effects of estrogen on the production of LH along with both a positive and negative feedback network can result in a nonlinear trigger mechanism with a high degree of variability and nonstationarity. Observed high variability in the length of the follicular phase is consistent with this type of nonlinear effect.

High levels of LH trigger ovulation and the transformation of the dominant mature follicle into the corpus luteus. The corpus luteus begins to produce progesterone and soon progesterone levels begin to rise. Progesterone in turn suppresses estrogen production and estrogen levels begin to fall. Once estrogen levels fall sufficiently, receptor–β turns off and receptor–α quickly suppresses production of LH. The slow surge in progesterone continues either until fertilization results or menstrual bleeding flushes the corpus luteum from the uterus and the cycle begins again.

Modeling Constraints

At this point, it is useful to list the modeling constraints and integrate them into a plan for building the differential equations model. Two types of constraints will be used: what we know from biology that would help make the model biologically plausible and what we know from repeated measures data: the plots of the daily assay data and the large scale studies' aggregated mean curves. The differential equations will be constructed to satisfy the following eight constraints:

1. Menstruation occurs approximately once every 29 days and lasts approximately 5 days.

2. Estradiol increases after menstruation. It may be that menstruation suppresses estradiol production. It takes about 15 days for estradiol to reach its peak.

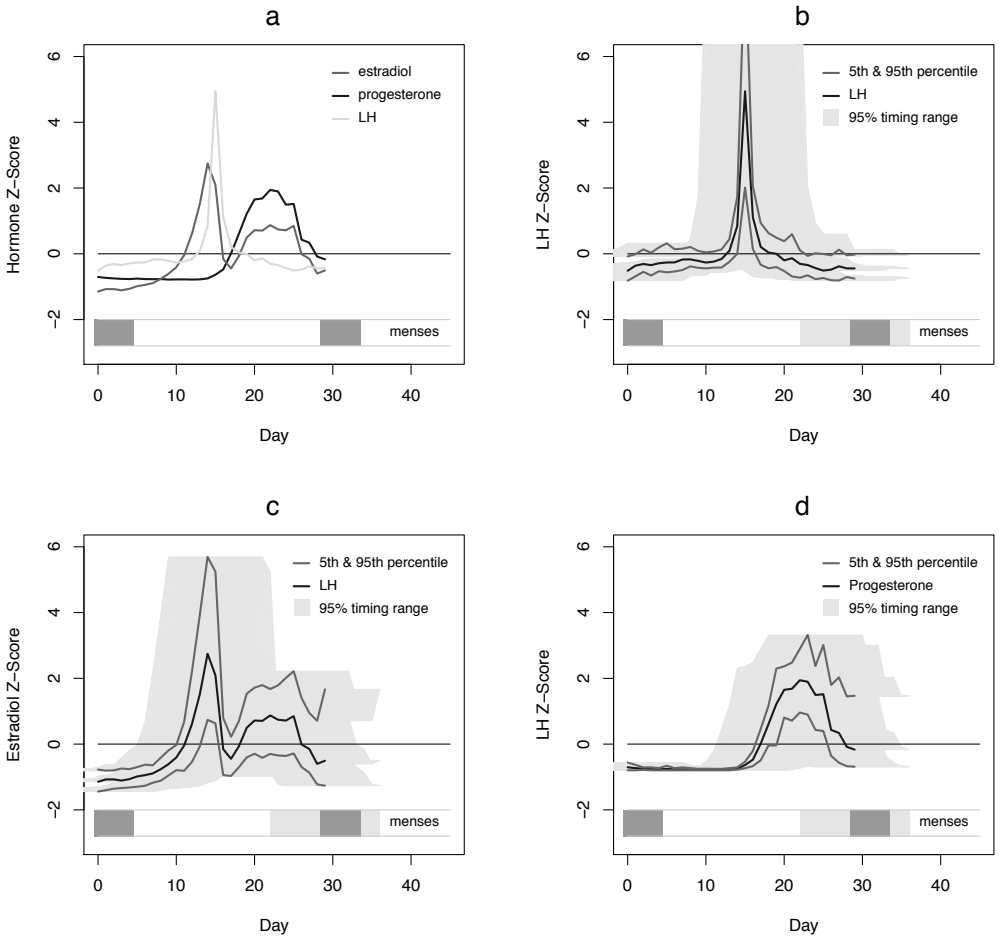

Figure 6. Visualization of (b) luteinizing hormone (LH), (c) estradiol, and (d) progesterone cycles. Shaded gray areas represent the 95% confidence intervals for the timing of the mean and percentile curves and onset of subsequent menses as referenced from onset of menses at day 0. All mean curves are referenced to the day of peak LH. Means, 5th, and 95th percentiles are from Stricker, et al. (2006) and timing variability estimates are from Fehring, et al. (2006).

3. LH production is suppressed when estradiol is below a threshold.

4. When estradiol is above a threshold (possibly the same threshold), LH then enters a positive feedback production cycle.

5. Progesterone production is triggered by LH.

6. Estradiol production is suppressed by progesterone.

7. From the data, estradiol levels drop more rapidly than could be explained by the slower increase in progesterone. One possible mechanism is that the LH pulse itself suppresses estradiol levels.

8. From the data, it appears that there is a fast (approximately 5 day) cycle in the estradiol levels after the LH pulse. This could be a result of a self–regulatory mechanism in estradiol production.

Model Specification

By choice, the modeling constraints did not attempt to explain onset or length of menses. While this is also an interesting problem, it is outside the scope of the example study, for which a model of estradiol and progesterone regulation is of primary interest. However, the data are consistent with menses having a suppression effect on estradiol. Thus, a discrete daily time series Z was constructed coded such that -1 represented days of menstrual bleeding and 0 for all other days. The variable $z(t)$ was then used as an exogenous variable in the model.

From the data, estradiol appears to have two oscillations: a slow oscillation and a fast oscillation that is only apparent after the LH pulse. As a first approximation, the model for estradiol levels was decomposed into two independent self–regulating oscillating systems: a slow oscillation with a period of about 30 days and a fast oscillation with a period of about 5 days. The slow estradiol equation was modeled as a damped linear oscillator with additional damping from menstrual bleeding and progesterone such that

$$\ddot{x} = \eta_x x + \zeta_x \dot{x} + \gamma_{xz} z + \gamma_{xp} \dot{p} \,, \tag{5}$$

where x, $\dot{x}$, and $\ddot{x}$ are the level, first and second derivatives of estradiol, z is -1 during menstrual bleeding and zero otherwise, and $\dot{p}$ is the first derivative of progesterone. The first derivative of progesterone was used since the biological constraint is that progesterone level reduces estradiol production (i.e., the first derivative of estradiol) and so by taking the first derivative of this relationship, we come up with a relationship between the second derivative of estradiol and the first derivative of progesterone.

Similarly, the fast estradiol oscillation was modeled as a damped linear oscillator with a trigger from the LH pulse as

$$\ddot{y} = \eta_y y + \zeta_y \dot{y} + \gamma_{yv} v \tag{6}$$

where y, $\dot{y}$, and $\ddot{y}$ are the level, first and second derivatives of the residuals of estradiol after the slow estradiol oscillation is taken into account, and v is the level of LH.

Progesterone was modeled as an overdamped second order linear system triggered by the LH pulse. This means that the progesterone was considered to be self–regulating once its cycle was initiated by the LH pulse. Thus, progesterone also takes the form

$$\ddot{p} = \eta_p p + \zeta_p \dot{p} + \gamma_{pv} v \tag{7}$$

where p, $\dot{p}$, and $\ddot{p}$ are the level, first and second derivatives of the residuals of progesterone, and v is the level of LH. Note that although this equation has the same form as Equations 5 and 6, the parameters η_p ad ζ_p are chosen so that damping occurs within the first cycle and so it is not considered to be an oscillator, but rather as an overdamped system.

Finally, the LH pulse was modeled. We did not have access to individual level LH data since the example study (Klump et al., 2013) did not assay LH levels. Thus, the only data constraint on LH comes from published aggregated average LH levels (Stricker et al., 2006). However, we do have more information about the mechanisms of the LH pulse. A reasonable assumption is that neural receptors with thresholds respond according to a sigmoid function. With that in mind, we first developed two sigmoid response functions, one for the estrogen receptor–α and one for the estrogen receptor–β. Each of these were modeled to respond to the sum of the slow and fast oscillation estradiol equations and were offset from each other so that the estrogen receptor–α stopped firing at estrogen levels slightly below the levels where the estrogen receptor–β began to fire. The two sigmoids thus were modeled as

$$\alpha = 1/(1 + e^{8(x+y+.5)}) \quad (8)$$

$$\beta = 1/(1 + e^{-10(x+y+.5)+3}) \quad (9)$$

where x and y are the slow and fast estradiol levels respectively. Note that the slope of β is a bit steeper than that of α and that β has an offset of 3 from the response point of the α. These effects are depicted graphically in Figure 7. The choice of the constants in these equations is somewhat arbitrary, but is constrained by the need for their combined response to approximate the published average LH curves.

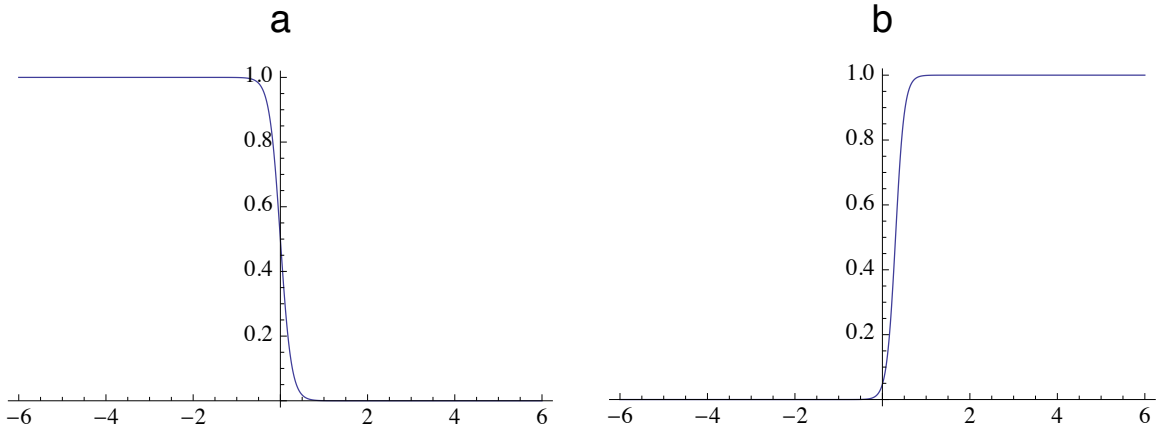

Figure 7. Sigmoidal response curves for the (a) estrogen receptor–α, (b) estrogen receptor–β.

The LH pulse was then modeled using a first order nonlinear system as

$$\dot{v} = \zeta_v v + \rho_\alpha \alpha v + \rho_\beta \beta v + \gamma_v p v + 0.01 \quad (10)$$

where v, $\dot{v}$, and $\ddot{v}$ are the level, first and second derivatives of LH, α and β are the two estrogen receptor responses, and p is the progesterone level. There are two parts to this

equation that are speculative, but were found to be necessary in order to reproduce the published average LH pulse. The equation thus makes two predictions that for which were were unable to find either positive or negative evidence. First, LH is considered to be self–damped, essentially hypothesizing a depletion model for production of LH in the hypothalmus, the prediction is that a large production of LH produces a refractory period in which LH production is more difficult to stimulate. This is not an implausible hypothesis, but the authors know of no positive evidence to support it. The second hypothesis is that there is a negative interaction between LH and progesterone such that when LH and progesterone are both high, LH production is suppressed. This second hypothesis is on less firm ground, but could be empirically tested.

Substituting the response curves for α and β into Equation 10 we now have a system of four simultaneous differential equations,

$$\begin{aligned}
\ddot{x} &= \eta_x x + \zeta_x \dot{x} + \gamma_{xz} z + \gamma_{xp} \dot{p} \\
\ddot{y} &= \eta_y y + \zeta_y \dot{y} + \gamma_{yv} v \\
\ddot{p} &= \eta_p p + \zeta_p \dot{p} + \gamma_p v \\
\dot{v} &= \zeta_v v + \rho\alpha v/(1 + e^{8(x+y+.5)}) + \\
&\quad \rho\beta v/(1 + e^{-10(x+y+.5)+3}) + \gamma_v p v + 0.01 \, ,
\end{aligned} \tag{11}$$

which can be numerically integrated to predict levels of each hormone over multiple cycles.

Simulated Time Series

We used the data from the individual plotted in Figures 1–c, 2–c, and 3–c as a target and hand tuned the coefficients of the simultaneous equations to approximate this individual's data as well as the average LH pulse shown in Figure 6–b. This procedure resulted in the constant coefficients substituted into the simultaneous equations as

$$\begin{aligned}
\ddot{x} &= -0.06x - 0.1\dot{x} + 0.2z \\
\ddot{y} &= -1.1y - 0.3\dot{y} + -0.1v \\
\ddot{p} &= -0.06p - .35\dot{p} + 0.1v \\
\dot{v} &= -3.5v - 1.5v/(1 + e^{8(x+y+.5)}) + \\
&\quad 4v/(1 + e^{10(-x-y+.5)+3}) - 0.1pv + 0.01 \, .
\end{aligned} \tag{12}$$

The system of equations in Equation 12 were numerically integrated using Mathematica (*Mathematica 8.0*, 2012) and the resulting trajectories from each equation are plotted in Figure 8 for an interval of 90 days. Note that the slow estradiol (Figure 8–b) and fast estradiol (Figure 8–c) are added together to form the predicted estradiol levels in Figure 8–d.

There are minor differences between the first cycle in, for instance Figures 8–d and –f, and the subsequent two cycles. That is because there is some carryover in the dynamics from the previous cycle that is not captured in the arbitrary initial conditions used to start the system at time $t = 0$. For this reason, we extracted a 45 day segment of the simulated estradiol and progesterone time series starting at day 38 of the simulation, in order to align the onset of menses in the simulation with the participant's data from Figures 1–c, 2–c. The simulated 45 day time series and observed time series for the participant are shown side–by–side for comparison in Figure 9.

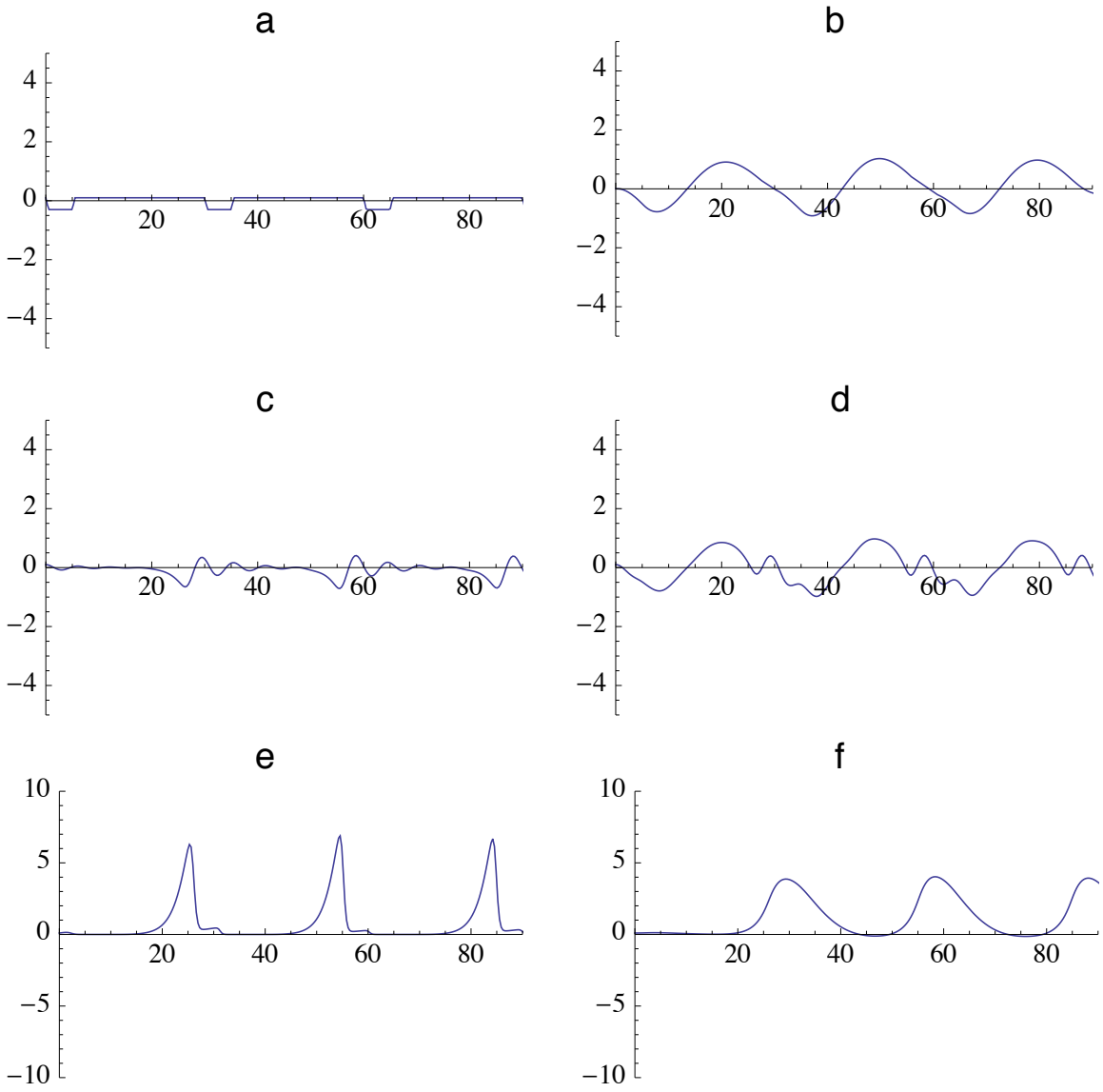

Figure 8. Simulated 90 day time series for (a) menses discrete time series, (b) slow estradiol cycle levels, (c) rapid estradiol cycle levels, (d) combined estradiol levels, (e) LH levels, (d) progesterone levels.

The simulated and observed time series share a number of similar features. However, the simulated time series is more smooth and the hormone peaks are more spread out. In addition, the simulation shows more fast oscillation in estradiol than does the observed time series. The spread nature of the hormone peaks in the simulated time series translate into a smoother autocorrelation function plot that de–emphasizes the secondary oscillation in estradiol.

Most important are similarities between the phase space plots. These plots allow the relationships between the derivatives of the simulated time series to be compared to the relationships between the derivatives of the observed time series. Most features of the observed phase space plot are captured in the phase space plot of the simulated time series. Note the relationships between the derivatives of progesterone — while the observed time series is a bit more noisy, the phase portrait shapes are very well preserved. There is also a striking similarity between the geometric shapes of the phase space of the simulated estradiol derivatives and the observed estradiol derivatives. The least similar are the coupled relationships between the estradiol derivatives and the progesterone derivatives. While many of the basic geometric features are similar, e.g., figure eights remain figure eights and loops remain loops, the details of the shapes are not as well preserved between simulated and observed as they were in the within–hormone dynamics.

Discussion

The aim of this chapter was to show how a complicated dynamical systems model with nonlinear components could be constructed. The process first used graphical display of a few individual time series in order to identify features that would need to be included in the model. Then, other information that was known about the system, from biology and from aggregate data was included in order to place constraints on the model design. An integrated list of model constraints was created and then the model was built step–by–step in order to satisfy these constraints. When the observed time series were not well explained by the biological constraints, new mechanisms were hypothesized and implemented so that the model could reproduce the major features of the data.

The model appears to be able to reproduce at least the major features of the dynamics observed in the individual–level time series — the primary aim of model construction. The next step will be to use model parameter estimation techniques, e.g., latent differential equations (Boker, Neale, & Rausch, 2004), to find maximum likelihood coefficients for the system of differential equations that can account both for within–person dynamics and between–persons individual differences. The results of this modeling effort will then inform models of coupling between daily self–report behavioral variables, such as eating and affect, and the hormone dynamics.

The results presented in this chapter are only a feasibility demonstration. The model includes several hypothesized biological mechanisms for which there is no evidence. There are two possible reasons for this mismatch. First, the model may just be wrong and the data features that we attempted to reproduce in one way perhaps could be reproduced in another way that did not require the novel hypothesized mechanisms. Alternatively, it could be that one or more of these biological mechanisms have not yet been discovered and that the model is pointing to areas for fruitful biological research in ovarian hormone regulation. At the

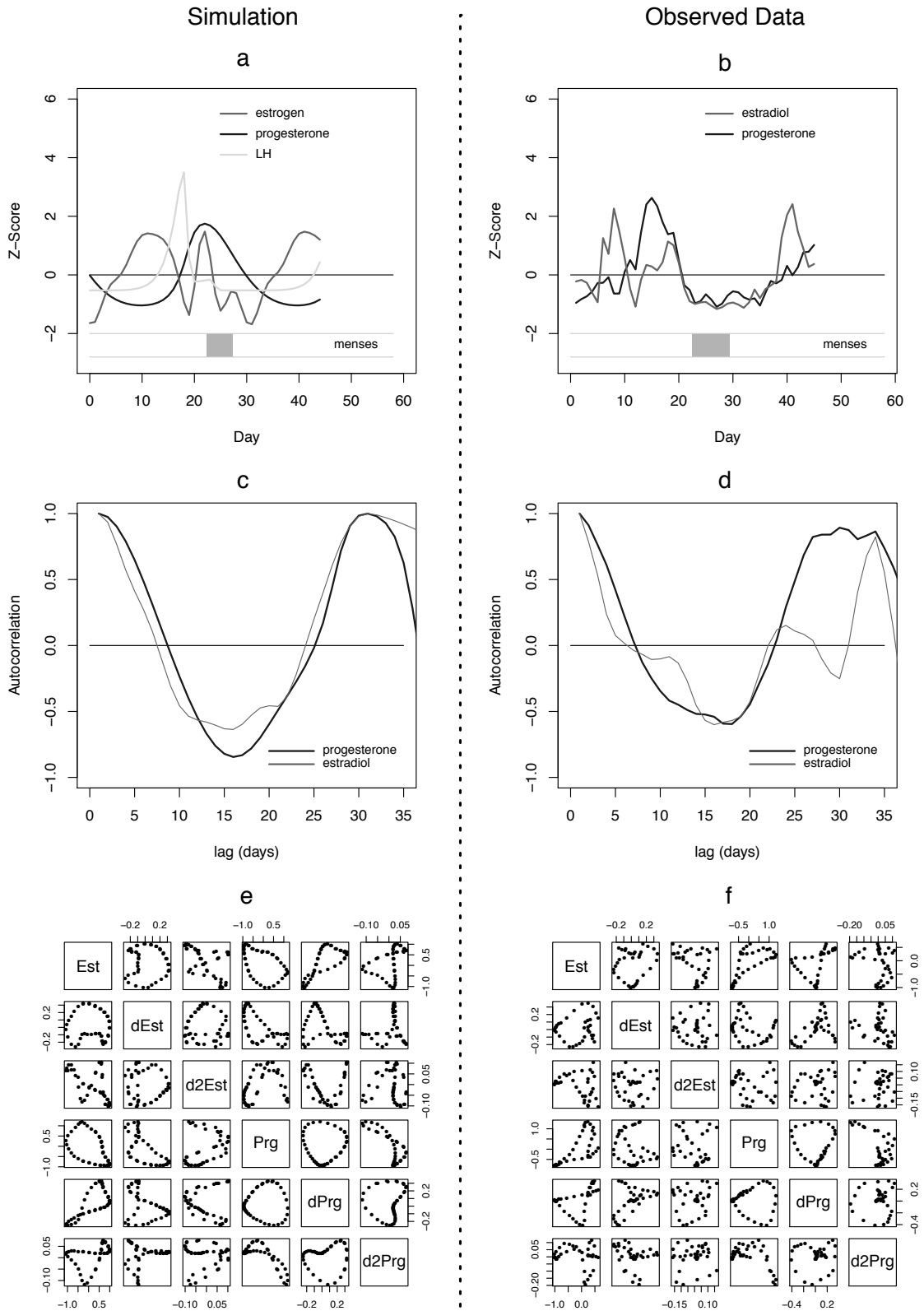

Figure 9. Comparison of 45 days of simulated data and one study participant's observed data using (a, b) time series, (c, d) autocorrelation functions, and (e, f) phase space reconstruction.

very least, by mathematically specifying a regulatory model using differential equations, a conversation can begin about features in the data that are not currently well–explained.

One interesting, but unintended consequence of the modeling described here is that the dynamics for the estrogen receptors α and β regulating the LH pulse produced a nonlinear instability that is consistent with high variability in the interval between the end of menses and the onset of ovulation but lower variability in the interval between ovulation and onset of subsequent menstrual bleeding. This difference in temporal variability was not part of the model design, but emerged from the dynamics as the biological constraints were implemented. We emphasize this point because when one is building and testing dynamical systems models, one should be alert to recognize emergent consequences of the model — both for positive explanatory purposes but also as a way of excluding parts of a model that produce behavior inconsistent with observations.

Conclusions

Differential equations models have the potential to provide explanatory power for understanding the dynamics of individuals' regulation of physiology, behavior and development. The model building process described in this chapter could be equally well be applied to daily diary data, ecological momentary assessment data, or long–term developmental data playing out over periods of decades. Building and fitting these models helps refocus research away from descriptions of what happened on average to a person–centered inquiry about how a system would behave given a particular context and current state. The study of human dynamics should aim for models of *how and why* rather than just models of *what*.

Appendix A

```
# ------------------------------------------------------------------------
# Program: MatrixPlotHormoneDerivatives.R
#  Author: Steven M. Boker
#    Date: Thu Dec 13 11:53:05 EST 2012
#
# This program is an example of how to create a matrix plot of
#   calculated derivatives from time series.
# The two functions that are read in may be obtained from the author's
#   website at
#   http://people.virginia.edu/~smb3u/GLLAfunctions.R
#   http://people.virginia.edu/~smb3u/GOLDestimates.R
# The simulated data can also be obtained from the same website:
#   http://people.virginia.edu/~smb3u/symOvarianSystem120913.csv
# This script can be downloaded at
#   http://people.virginia.edu/~smb3u/MatrixPlotHormoneDerivatives.R
#
# ------------------------------------------------------------------------

# ------------------------------------------------------------------------
```

```
# Read libraries and set options.

options(width=130)
source("GLLAfunctions.R")
source("GOLDestimates.R")
library(psych)

# ------------------------------------------------------------------------
# Set constants.

theDeltaT <- 1
embedD <- 11
theTau <- 1

# ------------------------------------------------------------------------
# Read the simulated from the chapter data.

simFrame1 <- read.table("symOvarianSystem120913.csv", header=FALSE, sep=",",
                col.names=c("day", "bleed", "slowEst", "dSlowEst", "fastEst",
                            "dFastEst", "LH", "dLH", "progest", "dProgest"))

describe(simFrame1)

# ------------------------------------------------------------------------
# Standardize variables and combine the slow and fast estradiol.

ZsimFrame1 <- data.frame(day=simFrame1$day,
                         bleed=simFrame1$bleed,
                         slowEst=scale(simFrame1$slowEst),
                         dSlowEst=scale(simFrame1$dSlowEst),
                         fastEst=scale(simFrame1$fastEst),
                         dFastEst=scale(simFrame1$dFastEst),
                         estradiol=scale(simFrame1$fastEst+.7*simFrame1$slowEst),
                         LH=scale(simFrame1$LH),
                         dLH=scale(simFrame1$dLH),
                         progest=scale(simFrame1$progest),
                         dProgest=scale(simFrame1$dProgest))

# ------------------------------------------------------------------------
# Time delay embed the three hormone variables.

embeddedEST <- gllaEmbed(ZsimFrame1$estradiol, embed=embedD, tau=theTau,
                         label="est", idColumn=FALSE)
embeddedPRG <- gllaEmbed(ZsimFrame1$progest, embed=embedD, tau=theTau,
                         label="prg", idColumn=FALSE)
```

```
embeddedLH <- gllaEmbed(ZsimFrame1$LH, embed=embedD, tau=theTau,
                        label="lh", idColumn=FALSE)

# ------------------------------------------------------------------------
# Combine first and last time-delay embedded columns into one matrix.

tEmbeddedMatrix <- cbind(embeddedEST[,c(1,embedD)], embeddedPRG[,c(1,embedD)],
                        embeddedLH[,c(1,embedD)])

# ------------------------------------------------------------------------
# Create a pdf of a 2-D state space plot for the three variables.

pdf(file=paste("MatrixPlot_StateSpace_Tau_11.pdf", sep=""), height=5, width=5)
pairs(tEmbeddedMatrix, cex=.25)
dev.off()

# ------------------------------------------------------------------------
# Estimate 0th, 1st, and 2nd derivatives for each variable.

wMatrix <- GOLDW(c(0:(embedD-1)),2)
gllaDataEST <- embeddedEST %*% wMatrix
dimnames(gllaDataEST) <- list(NULL, c("Est", "dEst", "d2Est"))
gllaDataPRG <- embeddedPRG %*% wMatrix
dimnames(gllaDataPRG) <- list(NULL, c("Prg", "dPrg", "d2Prg"))
gllaDataLH <- embeddedLH %*% wMatrix
dimnames(gllaDataLH) <- list(NULL, c("LH", "dLH", "d2LH"))


# ------------------------------------------------------------------------
# Merge estimated derivatives of all variables into a single data frame

gllaFrame <- data.frame(gllaDataEST, gllaDataPRG, gllaDataLH)
describe(gllaFrame)

# ------------------------------------------------------------------------
# Create a pdf of a phase space plot.

pdf(file=paste("MatrixPlot_PhaseSpace_D_11.pdf", sep=""), height=5, width=5)
pairs(gllaFrame, cex=.25)
dev.off()
```

References

Abarbanel, H., Brown, R., & Kadtke, J. (1990). Prediction in chaotic nonlinear systems: Methods for time series with broadband Fourier spectra. *Physical Review A*, *41*(4), 1782–1807.

Bisconti, T. L., Bergeman, C. S., & Boker, S. M. (2004). Emotion regulation in recently bereaved

widows: A dynamical systems approach. *Journal of Gerontology: Psychological Sciences*, *59*(4), 158–167.

Boker, S. M. (2012). Dynamical systems and differential equation models of change. In H. Cooper, A. Panter, P. Camic, R. Gonzalez, D. Long, & K. Sher (Eds.), *APA handbook of research methods in psychology* (pp. 323–333). Washington, DC: American Psychological Association.

Boker, S. M. (2013). Selection, optimization, compensation, and equilibrium dynamics. *GeroPsych: The Journal of Gerontopsychology and Geriatric Psychiatry*, *26*(1), 61–73.

Boker, S. M., Deboeck, P. R., Edler, C., & Keel, P. K. (2010). Generalized local linear approximation of derivatives from time series. In S.-M. Chow & E. Ferrar (Eds.), *Statistical methods for modeling human dynamics: An interdisciplinary dialogue* (pp. 161–178). Boca Raton, FL: Taylor & Francis.

Boker, S. M., Leibenluft, E., Deboeck, P. R., Virk, G., & Postolache, T. T. (2008). Mood oscillations and coupling between mood and weather in patients with rapid cycling bipolar disorder. *International Journal of Child Health and Human Development*, *1*(2), 181–202.

Boker, S. M., Molenaar, P. C. M., & Nesselroade, J. R. (2009). Issues in intraindividual variability: Individual differences in equilibria and dynamics over multiple time scales. *Psychology & Aging*, *24*(4), 858–862.

Boker, S. M., Montpetit, M. A., Hunter, M. D., & Bergeman, C. S. (2010). Modeling resilience with differential equations. In P. Molenaar & K. Newell (Eds.), *Learning and development: Individual pathways of change* (pp. 183–206). Washington, DC: American Psychological Association.

Boker, S. M., Neale, M. C., & Rausch, J. (2004). Latent differential equation modeling with multivariate multi-occasion indicators. In K. van Montfort, H. Oud, & A. Satorra (Eds.), *Recent developments on structural equation models: Theory and applications* (pp. 151–174). Dordrecht, Netherlands: Kluwer Academic Publishers.

Deboeck, P. R. (2010). Estimating dynamical systems: Derivative estimation hints from Sir Ronald A. Fisher. *Multivariate Behavioral Research*, *45*(4), 725–745.

Fehring, R. J., Schneider, M., & Raviele, K. (2006). Variability in the phases of the menstrual cycle. *Journal of Obstetric, Gynecologic & Neonatal Nursing*, *35*, 376–384.

Geirsson, R. T. (1991). Ultrasound instead of last menstrual period as the basis of gestational age assignment. *Ultrasound in Obstetrics & Gynecology*, *1*(3), 212–219.

Hu, L., Gustofson, R. L., Feng, H., Leung, P. K., Mores, N., Krsmanovic, L. Z., et al. (2008). Converse regulatory functions of estrogen receptor–α and –β subtypes expressed in hypothalamic gonadotropin–releasing hormone neurons. *Molecular Endocrinology*, *22*(10), 2250–2259.

Kennel, M. B., Brown, R., & Abarbanel, H. D. I. (1992). Determining embedding dimension for phase–space reconstruction using a geometrical construction. *Physical Review A*, *45*(6), 3403–3411.

Klump, K. L., Keel, P. K., Kashy, D. A., Racine, S., Burt, S. A., Neale, M., et al. (2013). The interactive effects of estrogen and progesterone on changes in binge eating across the menstrual cycle. *Journal of Abnormal Psychology*, *122*(1), 131–137.

Mathematica 8.0. (2012). Champaign–Urbana, IL: Wolfram Research.

Munster, K., Schmidt, L., & Helm, P. (1992). Length and variation in the menstrual cycle: A cross–sectional study from a danish county. *British Journal of Obstetrics and Gynecology*, *99*, 422–429.

Oertzen, T. v., & Boker, S. M. (2010). Time delay embedding increases estimation precision of models of intraindividual variability. *Psychometrika*, *75*(1), 158–175.

Ong, A. D., Bergeman, C. S., & Boker, S. M. (2009). Resilience in adulthood comes of age: Defining features and dynamic conceptions. *Journal of Personality*, *77*(6), 1777–1804.

Sauer, T., Yorke, J., & Casdagli, M. (1991). Embedology. *Journal of Statistical Physics*, *65*(3,4), 95–116.

Savitzky, A., & Golay, M. J. E. (1964). Smoothing and differentiation of data by simplified least squares. *Analytical Chemistry*, *36*, 1627–1639.

Stricker, R., Eberhart, R., Chevailler, M.-C., Quinn, F. A., Bischof, P., & Stricker, R. (2006). Establishment of detailed reference values for luteinizing hormone, follicle stimulating hormone, estradiol, and progesterone during different phases of the menstrual cycle on the abbott ARCHITECT analyzer. *Clinical Chemistry and Laboratory Medicine*, *44*(7), 883–887. (PMED ID: 16776638)

Takens, F. (1985). Detecting strange attractors in turbulence. In A. Dold & B. Eckman (Eds.), *Lecture notes in mathematics 1125: Dynamical systems and bifurcations* (pp. 99–106). Berlin: Springer–Verlag.

Whitney, H. (1936). Differentiable manifolds. *Annals of Mathematics*, *37*, 645–680.